Environment-Assisted Quantum Walks in Photosynthetic Energy Transfer

Environment-Assisted Quantum Walks in Photosynthetic Energy Transfer

Masoud Mohseni,[1] Patrick Rebentrost,[1] Seth Lloyd,[2] and Alán Aspuru-Guzik[1]

[1]*Department of Chemistry and Chemical Biology, Harvard University, 12 Oxford St., Cambridge, MA 02138*
[2]*Department of Mechanical Engineering, Massachusetts Institute of Technology, 77 Massachusetts Avenue, Cambridge MA 02139*

(Dated: May 23, 2008)

Energy transfer within photosynthetic systems can display quantum effects such as delocalized excitonic transport. Recently, direct evidence of long-lived coherence has been experimentally demonstrated for the dynamics of the Fenna-Matthews-Olson (FMO) protein complex [Engel *et al.*, Nature 446, 782 (2007)]. However, the relevance of quantum dynamical processes to the exciton transfer efficiency is to a large extent unknown. Here, we develop a theoretical framework for studying the role of quantum interference effects in energy transfer dynamics of molecular arrays interacting with a thermal bath within the Lindblad formalism. To this end, we generalize continuous-time quantum walks to non-unitary and temperature-dependent dynamics in Liouville space derived from a microscopic Hamiltonian. Different physical effects of coherence and decoherence processes are explored via a universal measure for the energy transfer efficiency and its susceptibility. In particular, we demonstrate that for the FMO complex an effective interplay between free Hamiltonian and thermal fluctuations in the environment leads to a substantial increase in energy transfer efficiency from about 70% to 99%.

PACS numbers: 03.65.Yz, 05.60.Gg, 71.35.-y, 03.67.-a

I. INTRODUCTION

Photosynthesis is the natural mechanism for the capture and storage of energy from sunlight by living organisms. Excitation energy is absorbed by pigments in the photosynthetic antennae and subsequently transferred to a reaction center where an electron-transfer event initiates the process of biochemical energy conversion. In certain bacterial systems and higher plants light harvesting efficiency is indeed above 99% [1]. Although this phenomenon has been studied for decades [2, 3, 4, 5], a full description of the underlying mechanism leading to this remarkably high efficiency is yet not available. It has already been demonstrated experimentally that the excitation energy transfer within chromophoric arrays of photosynthetic complexes could involve quantum coherence under certain physical conditions. In particular, this phenomenon has been observed via electronic spectroscopy of delocalized exciton states of light-harvesting complexes [2, 4] and the Fenna-Matthews-Olson (FMO) protein complex [5].

The energy transfer mechanism in multichromophoric arrays can often be described by a semiclassical Förster theory which involves incoherent hopping of the excitations between energy levels [6, 7, 8]. In this method, the Coulomb interaction among different sites is treated perturbatively to calculate the probability of exciton hopping. The more general approach for including coherent effects is given by Redfield theory which provides a microscopic description of excitation dynamics via a master equation in a reduced space of excitons in the weak phonon coupling and Born-Markov approximation [9]. An equivalent approach to Redfield theory for calculating the diffusion constant of excitons was proposed by Silbey and Grover [10]. Alternative methods to explore coherent and incoherent exciton transfer were also introduced using a stochastic model (Haken and Strobl [12]), and a generalized master equation formalism (Kenkre and Knox [13, 14]).

In order to study the nonlinear spectroscopy of molecular aggregates, Zhang *et al.* [15] introduced a modified Redfield equation for statically disordered exciton systems which treats the diagonal elements of exciton-bath coupling in a non-perturbative fashion. This approach was later used to model energy transfer dynamics in light-harvesting complexes of higher plants [4]. Yang and Fleming provide a comprehensive comparison of Förster, standard Redfield, and modified Redfield theories in Ref. [16]. A generalized theory for multichromophoric Förster resonance energy transfer which includes coherence effects within donors and acceptors, while considering donor-acceptor interactions according to the standard Förster model was also proposed by Jang, Newton, and Silbey [17, 18, 19]. In another study, the effects of geometry and trapping on energy transfer were examined in simple chromophoric arrays within the Haken-Strobl model [20]. Recently, direct evidence of quantum coherence in the dynamics of energy transfer has been observed experimentally in the FMO complex [21] and also in the reaction center of purple bacteria [22]. These previous studies led us to further explore and characterize quantum interference, decoherence effects, and their interplay within the dynamics of photosynthetic complexes as potential mechanisms for the enhancement of the energy transfer efficiency. Here, we develop a quantum walk approach, based on a quantum trajectory picture in the Born-Markov and secular approximations, as a natural framework for incorporating quantum dynamical effects in energy transfer, as opposed to a classical random walk picture that can effectively describe the excitation hopping in the Förster model.

The concept of quantum walks originated by Feynman works in connection with diffusion in quantum dynamics, in particular to model the dynamics of a quantum particle on a lattice [23], and also path integral formalism for discretizing the Dirac equation [24]. Continuous-time quantum walks were also used by Klafter and Silbey to find hopping time distribution functions in exciton dynamics [25]. The formal discrete and continuous-time approaches to quantum walks were developed later, e.g., see Refs. [26, 27], including some in-

vestigations of model decoherence effects [28]. Purely *unitary* continuous-time approaches to quantum walks were employed in the context of quantum information science, where they yield potential exponential speedups over classical algorithms [29, 30]. The quantum walks are of particular interest as potential computational tools [31], and applications to quantum cellular automata [32], quantum optical systems [33], and coherent excitation transport [34].

In this work, we develop a theoretical framework for studying the role of quantum coherence in energy transfer dynamics in molecular systems within the Born-Markov approximation in the Lindblad formalism. Our approach is essentially equivalent to a Redfield theory with the secular approximation. However, our approach naturally leads to quantum trajectory picture in a fixed-excitation reduced Hilbert space that can be described by the concept of directed quantum walks in Liouville space. Quantum walks in actual physical systems differ from idealized models of quantum walks in several significant ways. First, Hamiltonians of physical systems typically possess energy mismatches between sites that lead to Anderson localization [36]. Second, actual quantum walks are subject to relatively high levels of environment-induced noise and decoherence. The key result of this paper is that the interplay between the coherent dynamics of the system and the incoherent action of the environment can lead to significantly greater transport efficiency than coherent dynamics on its own. We introduce the concepts of energy transfer efficiency (ETE) and its susceptibility and robustness and explore the dynamical effects of coherent evolution and environmental effects at various temperatures from a microscopic Hamiltonian formalism. For the FMO protein, we show that a Grover-type quantum search [37] cannot explain the high ETE of this complex. However, we demonstrate that a directed quantum walk approach can be used for studying the energy transfer efficiency as a function of temperature, reorganization energy, trapping rate, and quantum jumps from sites to sites. Moreover, we explore similar dependencies for the susceptibilities of ETE with respect to basic processes contributing to the FMO dynamics including the free Hamiltonian, the phonon bath jumps, dephasing in the energy basis, transfer to the acceptor, and exciton decay. We demonstrate that the efficiency increases from 70% for a purely unitary quantum walk to 99% in the presence of environment-assisted quantum jumps.

This article is organized as follows. In Sec. II, we develop a Lindblad master equation in the site basis for studying energy transfer of multichromophoric channel systems in the Born-Markov approximation. In Sec. III, we introduce a quantum walks formalism in Liouville space to describe the energy transfer pathways. The definition of ETE is presented in Sec. IV. In Sec. V, we apply our theoretical approach for studying the dynamics of FMO complex. Some concluding remarks are given in Sec. VI.

II. LINDBLAD MASTER EQUATION FOR MULTICHROMOPHORIC SYSTEMS

The Fenna-Matthews-Olson protein acts as an energy transfer channel in the biological process of photosynthesis connecting the base plate of the antenna complex to the reaction center of green sulfur bacteria. This type of functional role of an interacting multichromophoric system can be formalized by the Hamiltonian for an consisting of N_D donors, N_C channel chromophores, and N_A acceptors as:

$$H_S = \sum_{m=1}^{N} \epsilon_m a_m^\dagger a_m + \sum_{n<m}^{N} V_{mn}(a_m^\dagger a_n + a_n^\dagger a_m). \quad (1)$$

The $a_m^\dagger$ and a_m are the creation and annihilation operators for an electron-hole pair (exciton) at chromophore m and ϵ_m are the site energies (not including the BChl a transition frequency 12500cm^{-1}) and $N = N_D + N_C + N_A$. The V_{mn} are Coulomb couplings of the transition densities of the chromophores, often taken to be of the Förster dipole-dipole form, $V_{mn} \sim \frac{1}{R_{mn}^3}(\mu_m \cdot \mu_n - \frac{3}{R_{mn}^2}(\mu_m \cdot \mathbf{R}_{mn})(\mu_m \cdot \mathbf{R}_{mn}))$, with $\mathbf{R}_{mn}$ the distance between site m and n and μ_m the transition dipole moment of chromophore m [2]. Note that in systems where chromophores are closely packed (e.g., the FMO complex of green sulfur bacteria [21]) or the site energies are (almost) resonant (e.g., the LH1 ring of purple bacteria [2]), ϵ_m can be of the same order of magnitude as V_{mn}. Such cases require a non-perturbative treatment of the coupling. In this work, the V_{mn} include all intra-donor/channel/acceptor couplings and inter-chromophoric couplings for donor-channel and channel-acceptor. Here, we ignore the V_{mn} for inter donor-acceptor coupling due to large spatial separation, as for example chlorosomes and reaction center in the green sulfur bacteria [38]. Thus, excitation transfer from donor to acceptor always occurs via the channel. We also assume that for donor-channel and channel-acceptor coherent couplings are weak, i.e., $V_{mn} \ll \epsilon_m$ for couplings into and out of the channel. This implies that the energy transfer to and from the channel can be described by semi-classical Förster theory.

In this work, we study the role of the FMO protein acting as an energy transfer channel in green sulfur bacteria. Thus, we focus on the dynamics of a chromophoric channel of N_C sites with denoting the free Hamiltonian in the reduced channel Hilbert space as H_C. The Hamiltonian H_C is formally equivalent to the Hamiltonian of Eq. (1) with $N = N_C$. We consider only the zero and single excitation manifolds given by the states $|0\rangle$ and $|m\rangle = a_m^\dagger|0\rangle$. We denote the eigenbasis of the Hamiltonian H_C as exciton basis $|M\rangle = \sum_m c_m(M)|m\rangle$, where $H_C|M\rangle = \epsilon_M|M\rangle$. Here, the effect of the donor is modeled by a static initialization of the channel. To account for the channel-acceptor coupling we introduce an effective non-Hermitian channel-acceptor Hamiltonian, $-iH_{C\to A} = -i\sum_{m=1}^{N_C} \kappa_m a_m^\dagger a_m$, which can be obtained by a projector-operator method analogous to Ref. [39], with the acceptor transfer rates $\kappa_m = 2\pi \int d\epsilon_a \, |V_{ma}|^2 \, \delta(\epsilon_m - \epsilon_a) D(\epsilon_a)$, where $D(\epsilon_a)$ denotes the density of states for the acceptor.

In general, the multichromophoric channel is subject to a thermal phonon bath and a radiation field. The interaction

Hamiltonian can be written as $H_I = H_p + H_r$, with the phonon coupling

$$H_p = \sum_{m,n}^{N_C} q^p_{mn} a^\dagger_m a_n, \tag{2}$$

where q^p_{mn} is an operator acting in the bath Hilbert space. The exciton-phonon and exciton-thermal photon interaction H_r describes the coupling of the bath operators q^r_m to the transition dipole moment of each chromophore, i.e.,

$$H_r = \sum_{m}^{N_C} q^r_m (a^\dagger_m + a_m). \tag{3}$$

The phonon terms $q^p_{mn} a^\dagger_m a_n$ induce relaxation and dephasing without changing the number of excitations. In other words, the state of the multichromophoric system remains in a fixed excitation manifold under the evolution generated by H_p. The H_r Hamiltonian leads to transitions between exciton manifolds. Generally, one can also consider diagonal static disorder in the Hamiltonian as: $H_d = \sum_{m=1}^{N_C} \delta\epsilon_m a^\dagger_m a_m$. This disorder can be generated for example by variation in the structure of the protein environment in the time scales which are usually much slower than excitation transfer time scale of ~ 1 ps [42].

The dynamics of the system to second order in the system-bath coupling, can be described by the Lindblad master equation in the Born-Markov and secular approximations as [40]:

$$\frac{\partial \rho(t)}{\partial t} = -\frac{i}{\hbar}[H_C + H_{LS}, \rho(t)] + L_p(\rho(t)) + L_r(\rho(t)). \tag{4}$$

where H_{LS} are the Lamb shifts due to phonon and photon-bath coupling. The respective Lindblad superoperators L_p and L_r are given by ($k = p, r$):

$$\begin{aligned} L_k(\rho) \;=\; & \sum_{\omega} \sum_{m,n} \gamma^k_{mn}(\omega)[A^k_m(\omega)\rho A^{k\dagger}_n(\omega) \\ & -\frac{1}{2} A^k_m(\omega) A^{k\dagger}_n(\omega)\rho - \frac{1}{2}\rho A^k_m(\omega) A^{k\dagger}_n(\omega)], \end{aligned} \tag{5}$$

For H_p the corresponding Lindblad generators are $A^p_m(\omega) = \sum_{\Omega-\Omega'=\omega} c^*_m(M_\Omega) c_m(M_{\Omega'}) |M_\Omega\rangle\langle M_{\Omega'}|$, where the summation is over all transitions with frequency ω in the single-excitation manifold and $|M_\Omega\rangle$ denotes the exciton with frequency Ω. The secular approximation is valid when the relevant time scale of the intrinsic evolution of the system, $\frac{1}{|\omega-\omega'|}$, is much faster than the relaxation time scale. For example, an energy difference of 200cm^{-1} between excitons, e.g., in the FMO complex, translates to a time scale of 0.16 ps which is much smaller than the typical 1 ps time scale of energy relaxation in the single-excitation manifold. The rates γ^p_{mn} are given by the Fourier transform of the bath correlation function as $\gamma^p_{mn}(\omega) = \delta_{mn} \int dt e^{i\omega t} \langle q^p_{mm}(t) q^p_{mm}(0)\rangle$, where we assume that off-diagonal fluctuations are small compared to diagonal fluctuations [5]. The rate can be further simplified to the site-independent expression $\gamma^p(\omega) = 2\pi[J(\omega)(1 + n(\omega)) + J(-\omega)n(-\omega)]$ where $n(\omega) = 1/[\exp(\frac{\hbar\omega}{kT}) - 1]$ is the bosonic distribution function at temperature T. Here, we assume an Ohmic spectral density with $J(\omega) = 0$ for $\omega < 0$ and $J(\omega) = \frac{E_R}{\hbar}\frac{\omega}{\omega_c}\exp(-\frac{\omega}{\omega_c})$ elsewhere, with cutoff ω_c, and reorganization energy $E_R = \hbar\int_0^\infty d\omega \frac{J(\omega)}{\omega}$ [5].

In the case of the Hamiltonian H_r we obtain the Lindblad generators $A^r_m(\omega_M) = c_m(M)|0\rangle\langle M|$, where $\hbar\omega_M = E_{Q_Y} + \epsilon_M$ is the molecular transition frequency, separated into $E_{Q_Y} \sim 12500\text{cm}^{-1}$ for the Q_Y band of bacteriochlorophyll a and excitonic energies ϵ_M of the order of 300cm^{-1} [42]. The respective rate is again assumed to be diagonal, $\gamma^r_{mn}(\omega) = \delta_{mn}\,\gamma^r_{mm}(\omega)$, and site independent, $\gamma^r_{mm}(\omega) = \gamma^r(\omega)$. For Ohmic $\sim \omega$ and super-Ohmic spectral densities one is able to approximate $\gamma^r((E_{Q_Y} + \epsilon_M)/\hbar) \approx \gamma^r(E_{Q_Y}/\hbar)$. This approximation yields a simplified Lindblad superoperator similar to Eq. (5) without the summation over frequencies and with the generators $A^r_m = |0\rangle\langle m|$. Finally, we choose the rates $\gamma^r(\omega)$ such that it leads to a 1ns exciton life-time, as experimentally measured for chromophoric complexes e.g., in Ref. [41]. The Lamb-shifts $H_{LS} = H^p_{LS} + H^r_{LS}$ are explicitly given by $H^k_{LS} = \sum_{\omega,n,m} S^k_{nm}(\omega) A^{k\dagger}_n(\omega) A^k_m(\omega)$ (for $k = p, r$) where $S_{nm}(\omega)$ is the imaginary part of the half-sided Fourier-transform of the bath-correlator. The Lamb shift usually contributes only marginally to the dynamics of the system, e.g. in the FMO complex [42].

The master equation Eq. (4) and its Lindblad superoperators Eq. (5) contain a significant degree of complexity, reflecting the non-trivial form of the FMO complex and its diverse sources of environmental interaction. To deal with this complexity one needs to separate the contributions of the different physical processes to the dynamics. To this end, in the next section, we explicitly construct a quantum trajectory master equation to study the effects of free Hamiltonian, damping and relaxation. Specifically, we demonstrate that the energy transfer in multi-chromophoric systems of the chromophoric channel can be considered as a generalized (directed) continuous-time quantum walk in the single-excitation manifold interrupted by jumps to the zero-excitation manifold.

III. QUANTUM WALK FORMALISM FOR ENERGY TRANSFER

In general, the Förster theory for energy transfer leads to a classical random walk description of the transport in photosynthetic units [43, 44]. The equation of motion for the classical probabilities of an excitation being at site a, P_a, is given by

$$\frac{\partial P_a(t)}{\partial t} = \sum_{b=1}^{N_C} M_{ab} P_b(t). \tag{6}$$

The M_{ab} denotes the Markov transition matrix elements which describes the classical Förster rates between site a and b. In closely-packed chromophoric arrays, however, one has to consider not only populations of states but also coherence between states; consequently, the equation of motion is given

by a master equation for the density matrix such as Eq. (4). For the purposes of evaluating the dynamics of this master equation, and for investigating the interplay between coherence and decoherence in the resulting quantum walk, it is convenient to re-express the master equation for a single excitation in terms of a quantum trajectory picture of open quantum system dynamics, as in [45, 46]:

$$\begin{aligned}\frac{\partial\rho(t)}{\partial t} &= -\frac{i}{\hbar}[H_{eff},\rho(t)]^{\star} \\ &+ \sum_{m,m',n,n'}^{N_C}\Gamma^{p}(m,m',n,n')W_{m,m'}\rho(t)W^{\dagger}_{n,n'} \\ &+ \sum_{m}^{N_C}\gamma^{r}_{m}R_{m}\rho(t)R^{\dagger}_{m},\end{aligned} \tag{7}$$

where the $W_{m,m'} = a^{\dagger}_{m}a_{m'}$ generate jumps in the single-exciton manifold and the $R_m = a_m$ generate jumps between exciton manifolds. The jump rates are given by $\Gamma^{p}(m,m',n,n') = \sum_{l,\omega}\gamma^{p}(\omega)\langle m|A^{p\dagger}_{l}(\omega)|m'\rangle\langle n|A^{p}_{l}(\omega)|n'\rangle$, and $\Theta^{p}(m,n) = \sum_{l,\omega}\gamma^{p}(\omega)\langle m|A^{p\dagger}_{l}(\omega)A^{p}_{l}(\omega)|n\rangle$. We have also defined $[,]^{\star}$ as a generalized commutation relation for any two operators A and B as $[A,B]^{\star} = AB - B^{\dagger}A^{\dagger}$. In order to describe absorption of the exciton at the acceptor site and the damping due to the phonon bath, we introduced an effective anti-Hermitian Hamiltonian as: $H_{eff} = H_C + H_{LS} + H_{decoher}$, with

$$\begin{aligned}H_{decoher} &= -\frac{i}{2}\{\sum_{m,n=1}^{N_C}\Theta^{p}(m,n)a^{\dagger}_{m}a_{n} \\ &+ \sum_{m}\sum_{\omega}\gamma^{r}_{m}(\omega)a^{\dagger}_{m}a_{m} + H_{C\rightarrow A}\}.\end{aligned} \tag{8}$$

Now taking the trace of the overall master equation leads to the probability density that no jump to the zero manifold occurs between time t and $t+dt$ as: $p_{no-jump} = -2i\mathrm{Tr}[H_{decoher}\rho_{eff}(t)]dt + \sum_{m,m',n,n'}^{N_C}\Gamma^{p}(m,m',n,n')\mathrm{Tr}[W_{m,m'}\rho_{eff}(t)W^{\dagger}_{n,n'}]dt$, and the probability density of a jump event becomes: $p_{jump} = \sum_{m}^{N_C}\gamma^{r}_{m}\mathrm{Tr}[R_{m}\rho_{eff}(t)R^{\dagger}_{m}]dt$. In the case of a no-jump trajectory one has the master equation $\frac{\partial\rho_{eff}(t)}{\partial t} = -\frac{i}{\hbar}[H_{eff},\rho_{eff}(t)]^{\star} + \sum_{m,m',n,n'}^{N_C}\Gamma^{p}(m,m',n,n')W_{m,m'}\rho_{eff}(t)W^{\dagger}_{n,n'}$, which can be considered as a directed quantum walk on the one-exciton manifold described by the density operator ρ_{eff}.

We note that the contribution due to the free Hamiltonian, i.e., the equation $\frac{\partial\rho(t)}{\partial t} = -\frac{i}{\hbar}[H_C,\rho(t)]$ represents a continuous-time unitary quantum walk in the single-excitation manifold. The off-diagonal elements of the free Hamiltonian terms represent quantum coherent hopping with amplitudes $H_{C,mn}$ between the localized sites with energy $H_{C,mm}$. The analogy of continuous-time unitary quantum walks to classical random walks was addressed within the context of quantum algorithms in Ref. [29] and further explored in [27, 30]. The damping contribution to the dynamics within $-\frac{i}{\hbar}[H_{eff},\rho(t)]^{\star}$ leads to site-dependent relaxation for both diagonal and off-diagonal elements of the density operator and the terms $\sum_{m,m',n,n'}^{N_C}\Gamma^{p}(m,m',n,n')W_{m,m'}\rho(t)W^{\dagger}_{n,n'}$ induce quantum jumps in the single-excitation manifold.

The similarity between quantum walks and classical random walks, Eq. (6), can be readily emphasized in Liouville space. The quantum trajectory picture is re-expressed as a matrix equation by representing the density operator in a vectorial form. Thus, quantum walks in multi-chromophoric complexes are described by the equation

$$\frac{\partial\vec{\rho}_{a}(t)}{\partial t} = \sum_{b}\mathcal{M}_{ab}\vec{\rho}_{b}(t), \tag{9}$$

where $\vec{\rho}^{T}(t) = (\ \rho_{11}\ \ \rho_{12}\ \ \cdots\ \ \rho_{N_CN_C-1}\ \ \rho_{N_CN_C}\ )$. This equation manifests a quantum walk in the N_C^2-dimensional Liouville space, with the transition (super-) matrix,

$$\begin{aligned}\mathcal{M}_{ab} &= -\frac{i}{\hbar}\{I\otimes H_{eff} - H^{*}_{eff}\otimes I)_{ab} \\ &+ \sum_{m,m',n,n'}^{N_C}\Gamma^{p}(m,m',n,n')(W^{*}_{n,n'}\otimes W_{m,m'})_{ab}.\end{aligned} \tag{10}$$

The time variation of the vector $\vec{\rho}(t)$ in Liouville space represents the dynamics of population elements ρ_{mm} as well as coherence elements ρ_{mn}, which are the signature of quantum dynamics. The real part of $\mathcal{M}$ is responsible for the directionality in the quantum walk which enhances the excitation energy transfer for the FMO complex as we will demonstrate later. This is due to the *effective* interplay between the free Hamiltonian and phonon-bath coupling that generates quantum jumps. Next we study the properties of the quantum walk picture in terms of the energy transfer efficiency as an universal measure.

IV. ENERGY TRANSFER EFFICIENCY

The energy transfer efficiency of the channel is defined as the integrated probability of the excitation successfully leaving the channel to the acceptor. This definition of the channel efficiency has the advantage of being independent of the detailed dynamics within the acceptor, charge separation, and the energy storage via a chemical reaction. More formally we define:

$$\eta = \frac{1}{\hbar}\int_{0}^{\infty}\mathrm{Tr}(H_{C\rightarrow A}\rho(t))dt. \tag{11}$$

Similar definitions, using *integrated* success probabilities, were used in context of energy transfer from donor to acceptors [3, 46], and quantum random walks [30, 34]. Note that the efficiency in Eq. (11) has the upper limit of ∞, yet in most practical cases there is always a natural cutoff, $1/\gamma^{r}_{m}$, due to finite excitation life-time, e.g., for chromophoric complexes and GaAs quantum dots $1/\gamma^{r}_{m} \sim 1$ns [43, 47]. Moreover, the relevant dynamical time scale for the excitation to be

transferred to the acceptor is about $1/\kappa_m$. A more quantitative measure for the transfer time through the quantum channel to the acceptor is given by,

$$\tau = \frac{1}{\eta}\int_0^\infty t\,\mathrm{Tr}(H_{C\to A}\rho(t))dt. \tag{12}$$

In this work we mainly focus on the energy transfer efficiency. In order to study its optimality and robustness, we define a decomposition Λ_k of the superoperator by $\mathcal{M} = \sum_k \Lambda_k$.The different Λ_k can be chosen in any desired way in order to isolate the effect of different parts of the master equation. For example, one Λ_k could represent the effect of the system Hamiltonian on its own, while another could represent the effect of the phonon bath. Each term Λ_k is associated with a scalar quantity λ_k, which represents the overall strength of the of the kth term in the dynamics. For example, the λ_k associated with the Hamiltonian gives the overall energy scale of the Hamiltonian, while the λ_k associated with the photon bath gives the strength of the coupling to that bath.

It is natural to investigate the energy transfer efficiency in terms of the susceptibilities $\frac{\partial\eta}{\partial\lambda_j}$ and the Hessian $\frac{\partial^2\eta}{\partial\lambda_j\partial\lambda_k}$, using the scaling parameters $\Lambda_k \to \lambda_k\Lambda_k$, in the neighborhood of $\lambda_k \to 1$. For any chromophoric complex the gradient of the efficiency defined by the set of $\frac{\partial\eta}{\partial\lambda_j}$ can be used as a measure for local optimality of its performance with respect to independent parameters λ_k. Moreover, such efficiency gradient can be utilized for engineering photovoltaic materials with optimal and robust energy transfer in their respective parameter space. One can verify that the susceptibilities satisfy the identity $\sum_k \frac{\partial\eta}{\partial\lambda_k} = 0$, where the sum consists of a complete decomposition of the superoperator. This identity is the consequence of energy conservation for all times t: In the single-excitation manifold, the energy that is transferred by the physical processes $H_{C\to A}$ out of the chromophoric channel is absorbed by the reaction center in a given time interval. Additionally, the Hessian $\frac{\partial^2\eta}{\partial\lambda_j\partial\lambda_k}$ is a measure for the second-order robustness of natural or engineered chromophoric systems. Note that the robustness also satisfies a similar conservation property, i.e., $\sum_{j,k}\frac{\partial^2\eta}{\partial\lambda_j\partial\lambda_k} = 0$. Next, we study the quantum walk approach in the context the ETE in the FMO complex.

V. FENNA-MATTHEWS-OLSON COMPLEX

The structure of the Fenna-Matthews-Olson (FMO) complex of green sulfur bacteria was revealed by x-ray crystallography [38], as the first pigment-protein complex structure to ever be determined in this method, and since then it has been extensively studied [48]. The FMO complex consist of a trimer, formed by three identical monomers, each constituting of seven bacteriochlorophyll molecules (BChl a) supported by a rigid protein backbone. The FMO complex essentially acts as a molecular wire, transferring excitation energy from the chlorosomes, which are the main light-harvesting antennae of green sulfur bacteria, to the membrane-embedded type I reaction center. In the recent study of the *Chlorobium tepidum* FMO complex by Engel *et al.*, [21], using two-dimensional electronic spectroscopy, direct evidence of long-lived coherence in the form of quantum beatings was demonstrated at 77K. The presence of quantum coherence prompted speculations about the presence of quantum computation in FMO. Indeed, it was argued that FMO acts as a dedicated computational device [21], since excitons are able to explore many states simultaneously and select the correct answer, which here is the lowest energy excitonic state. This operation was claimed to be *analogous* to Grover's algorithm, which is known to provide a quadratic speed-up over its classical counterparts for searching elements of an unstructured database [37]. Here, we argue that a purely unitary Grover-type search algorithm cannot explain the efficiency of the exciton transfer in FMO complex. However, we employ our directed quantum walk approach to study the quantum effects in the dynamics of the FMO complex.

We use the free Hamiltonian of the FMO complex as given in Ref. [5]. The site-energy differences and inter-site couplings lead to exciton energies with separations of around $100\mathrm{cm}^{-1}$. The highest energy states are exciton 6 and 7 which are mainly delocalized over sites 5/6 and 1/2, respectively. The lowest exciton state 1 involves the site 3. For an overview of the structure of the FMO complex see Fig. 1 (a). The initial states for the simulation are taken to be sites 1 and/or 6 which are close to the chlorosome antenna (donor) [42]. Transfer of the excitation from the FMO channel to the acceptor occurs via site 3 with the rate κ_3, which is a free parameter in our simulations and, if not otherwise stated, taken to be $\kappa_3 = 1\mathrm{ps}^{-1}$. The exciton lifetime is assumed to be $1/\gamma^r = 1\mathrm{ns}$ [3, 41]. The bath spectrum is taken to be as described above with the reorganization energy $E_R = 35\mathrm{cm}^{-1}$ and cutoff $\omega_c = 150\mathrm{cm}^{-1}$, inferred from Fig. 2 of Ref. [42].

The purely unitary evolution generated by the seven-site Hamiltonian is not performing a Grover-type search. In general, for a unitary evolution to be qualified as a quantum search a certain set of conditions have to realized: (i) $\langle\psi_{ES}|\,\rho_i(t_0)\,|\psi_{ES}\rangle = 1-\alpha$, where $|\psi_{ES}\rangle = \frac{1}{\sqrt{N}}\sum_m |m\rangle$ is an equal superposition of the basis states $\{|m\rangle\}_{m=1}^N$ of the Hilbert space including the solution the search, the target state $|m^*\rangle$. $\rho_i(t_0) = |\psi_i(t_0)\rangle\langle\psi_i(t_0)|$ is the pure initial state of the system at some arbitrary time t_0 and $\alpha \ll 1$. For a standard Grover search algorithm α is equal to zero. This condition assures that the initial input state of the search is unbiased with respect to the target state. (ii) $\left|\langle m^*|\,e^{-i(t_f-t_o)H}\,|\psi_i(t_0)\rangle\right|^2 = 1-\beta$, where t_f is the smallest time in which the free evolution of the initial state, $e^{-i(t_f-t_o)H}\,|\psi_i\rangle$, has significant overlap with the target state, and $\beta \ll 1$. (iii) $t_f = \gamma\sqrt{N}$, where γ is either a constant or a $poly(\log N)$. In summary, a Hamiltonian generating the Grover algorithm should map an equal coherent superposition of all possible (database) states into a desired target state, within a time polynomial in the size of database and with a probability of close to one. For the FMO complex, we have investigated a variety of different reasonable initial states (e.g., an equal superposition of all BChl states, or a localized excitation on BChls 1 and 6) and target states (e.g., the state localized in BChl 3). In neither case did the

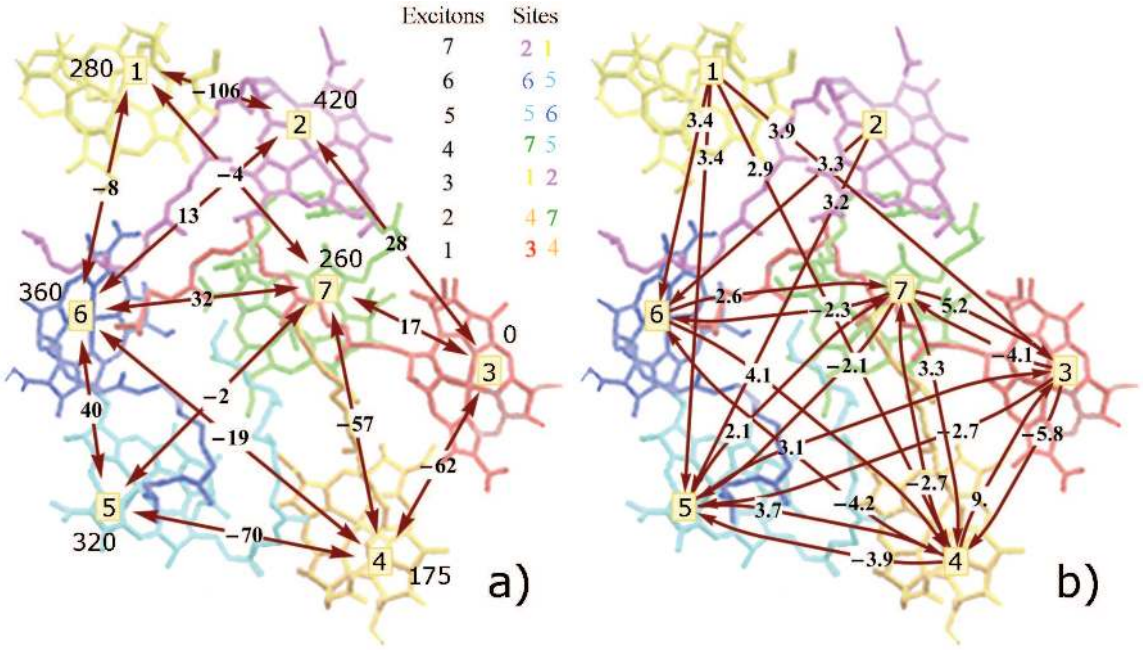

FIG. 1: The Fenna-Matthews-Olson protein: (a) The spatial structure and energy levels of the complex, where the number at each site represents the localized site energy and the arrows with numbers denote the couplings among various bacteriochlorophylls. For clarity, some small couplings are not shown. The inset depicts the participation of the seven chlorophylls in the delocalized excitonic states [5]. (b) The susceptiblities of energy transfer efficiency with respect to perturbations of inter-site jumps and corresponding damping, rescaled by a factor of 10^4 and drawn with a cutoff of 2.0. The initial state is taken to be a mixture of populations at site 1 and 6. Standard parameters are $E_R = 35\text{cm}^{-1}$, $T = 295\text{K}$, $\kappa_3 = 1\text{ps}^{-1}$, and $\gamma^r = 1\text{ns}^{-1}$. Susceptibilites are large when inter-chromophoric couplings are strong and site-energies are similar. The sign of the susceptibility is an indication of the directionality towards the target site 3.

coherent Hamiltonian dynamics result in a significant overlap to the target state. We found that the overlap oscillates in time but never exceeds the value of 0.4. We conclude that the *unitary* Grover search algorithm cannot explain the efficiency of the exciton transfer in FMO complex. However, in principle, certain non-unitary generalizations of quantum search algorithms could still be developed to be relevant in this context; especially for the case of non-unitary oracles interacting with a non-Markovian and/or spatially correlated environment.

We investigate other non-trivial quantum dynamical effects in the presence of phonon-bath fluctuations and exciton recombination and trapping. The results are shown in Figs. 1, 2, and 3. In Fig. 2 (a), we illustrate the functional dependence of the ETE, Eq. (11), on temperature for two initial states localized at site 1 or 6, respectively. The overall dependence is less than 1% for reasonable temperatures. This can be explained by the relatively small size of the FMO and the approximately three orders of magnitude separation of lifetime $(1/\gamma^r)$ and acceptor transfer $(1/\kappa_3)$ timescales. In order to see this, note that at zero temperature there are only quantum jumps originated from spontaneous emission of energy into the phonon bath, leading to relaxation down the energy funnel. This phenomenon in itself leads to a high efficiency of transport, due to the presence of irreversible trapping on a time scale much faster than the lifetime of the excitation. At higher temperatures quantum jumps due to stimulated emission and absorption enter the dynamics. Both processes have the same rates and a temperature dependence which is determined by the bosonic distribution function $n(\omega)$. In the FMO protein, stimulated emission of excitonic energy helps the transport, since the target state has the lowest energy. The effect of absorption is twofold: It facilitates the overlap with the trapping site when there is an energy barrier in the transport path. At the same time, absorption processes can lead to transfer away from low-energy target sites ("detrapping"). These effects explain the difference in the temperature dependence for the two initial states localized either at site 1 or at site 6. The ETE increases slightly with temperature for the initial state being at site 1 (blue line in Fig. 2 (a)). This site has a large overlap with exciton 3 and the spatial pathways to site 3 involve energetically higher excitons 4,5,6, and 7, see Fig. 1 (a). Detrapping explains the slight decrease of ETE as a function of temperature for initial state 6 (red line in Fig. 2 (a)). This site has a high overlap with exciton 5 and 6 and energetically funnels down to exciton 1 (site 3). For larger photosynthetic complexes and/or in the absence of low-energy trapping sites, the temperature dependence of the efficiency is expected to be more significant. First, temperature-independent spontaneous emission will play a less prominent role. Second, the energy transfer time will become more comparable to the exciton lifetime. This translates to a higher temperature dependence for the overall efficiency since any variation in the transport becomes more pronounced. mes.

The functional dependence of the ETE on the reorganization energy at room temperature is shown in Fig. 2 (b). The reorganization energy can be understood as a linear scaling of

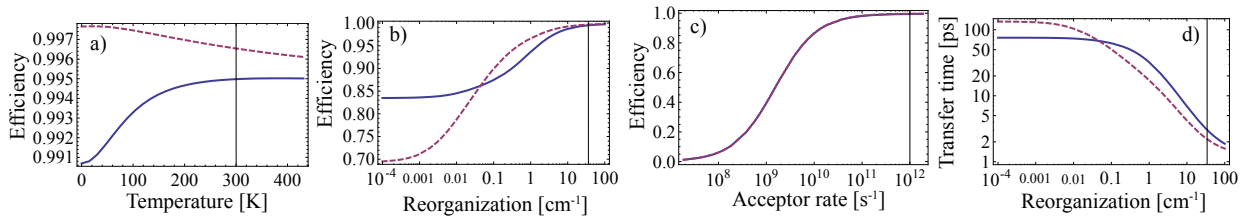

FIG. 2: Energy transfer efficiency as a function of a) temperature, b) reorganization energy (log-linear), and c) transfer rate to the acceptor (log-linear). Transfer time as a function of reorganization energy d). Blue lines show the efficiencies starting from an initial state localized at site 1. Red lines how the efficiencies starting from site 6. The default parameters (shown as vertical lines) are taken to be $T = 295$K, $\kappa_3 = 1\text{ps}^{-1}$, $\gamma^r = 1\text{ns}^{-1}$, and $E_R = 35\text{cm}^{-1}$. A quantum walk with no environment-assisted jumps corresponds to no reorganization energy in panel b). The energy transfer efficiency in this case is 15-30% less than for the parameters obtained experimentally for FMO demonstrating the effect of the environment-assisted quantum walk.

the phonon bath. Thus, at $E_{\rm R} = 0$ we have the (pure) quantum walk limit leading to efficiencies of 70% and 85% respectively for both pathways. The difference of 15% between the two different initial states can be explained by the higher localization of initial state 6 due larger energy mismatch of site 6 and target site 3**.** An increase in reorganization energy results in an efficiency increase up to about 99%, demonstrating the effect of the environment-assisted quantum walk.

As mentioned before the actual value of the irreversible transfer rate κ_3 from the FMO complex to the reaction center (acceptor) is not well known**,** since there exists insufficient chrystallographic data for the combined FMO/RC structure [38]. In Fig. 2 (c), we explore the dependence of the ETE on this unknown parameter at room temperature**.** The ETE increases monotonically from zero to almost one within a range of five orders of magnitude. One obtains the largest increase in efficiency when the acceptor transfer rate is $\sim 1\text{ns}^{-1}$ thus surpasses the lifetime rate γ^r. In the limit of large transfer rates to the acceptor, $\kappa_3/\gamma^r \gg 1$, the lifetime of the excitation does not significantly reduce the efficiency. On the other hand, in the limit of small transfer rates to the acceptor, $\kappa_3/\gamma^r \ll 1$, most of the excitation dissipates into the environment before being transferred to the acceptor.

Figure 2 (d), shows the transfer time, Eq. (12), of the excitation initially at site 1 or 6 to the acceptor as a function of reorganization energy. In the fully quantum limit it takes the excitation more than 50ps to arrive at the acceptor. This value dramatically improves for higher reorganization energies. At the value of $E_R = 35\text{cm}^{-1}$ one finds a transfer time of around 4ps^{-1}, which was reported based on different considerations in [42].

Figure 3 illustrates the susceptibilities $\frac{\partial \eta}{\partial \lambda_j}$ for the basic processes in the FMO dynamics including the Hamiltonian, the phonon bath coupling, transfer to the acceptor, and the loss of the excitation. In Fig. 3 (a), the susceptibilities for those processes are shown as a function of temperature. The susceptibility of the ETE to the phonon bath shows several interesting features. The system is rather susceptible to perturbations of the phonon bath coupling at zero temperature. In this limit, the directionality of the quantum walk is maximized, since, due to spontaneous emission, the excitation can only move down in energy towards the target site 3 while energy absorption from the phonon bath is suppressed. Increasing temperature leads to increased stimulated emission *and* absorption, thus the system is less susceptible to perturbations of the phonon bath since their effect on emission and absorption processes is the same. Concomitantly, the efficiency becomes more susceptible to the transfer process to the reaction center at higher temperature. This is again readily explained by the increased phonon-bath absorption rate: In the presence of detrapping processes it becomes more important to capture the excitation immediately once it arrives at site 3. We note that the efficiency is not susceptible to a small variation of the free Hamiltonian due to inherent irreversibility of the fully unitary quantum dynamics. The susceptibility with respect to dephasing in the energy basis has also insignificant variation for all the temperatures considered here due to the dominant role of the quantum jumps to the overall ETE, and thus is not presented in Fig. 3.

The dependence of the susceptibilities of the ETE as a function of the reorganization energy is shown in Fig. 3 (b). The susceptibility of the ETE to the phonon bath peaks at around 1cm^{-1} for the initial state 1 and around 0.01cm^{-1} for the initial state 6. Note that, for the Ohmic spectral density considered here, the reorganization energy scales linearly the strength of the coupling to the phonon bath, therefore this curve is the derivative of the ETE in Fig. 2 (b), where the steepest ascent occurs around 1cm^{-1} or 0.01cm^{-1} respectively. The susceptibility of the ETE on the transfer rate to the acceptor becomes smaller for higher reorganization energy. Larger reorganization energy leads to faster thermalization. In this regime the system is more resilient to perturbations of the transfer process to the acceptor and the dissipation to the environment.

The dependence of the susceptibility of the ETE on the acceptor transfer rate is illustrated in Fig. 3 (c). We observe a maximum in the susceptibility at around 1ns^{-1}, which is the regime where the time scales of transfer to the acceptor and the lifetime are comparable, $\kappa \sim \gamma^r$, compare to Fig. 2 (c).

The susceptibilities of the energy transfer efficiency on inter-site quantum jumps is shown in Fig. 1 (b). More formally, we look at the effect of perturbations of site to site jump terms and the corresponding damping, $\Lambda_{nm} = -\Theta^p(m,m)(I \otimes a_m^\dagger a_m + a_m^\dagger a_m \otimes I) +$

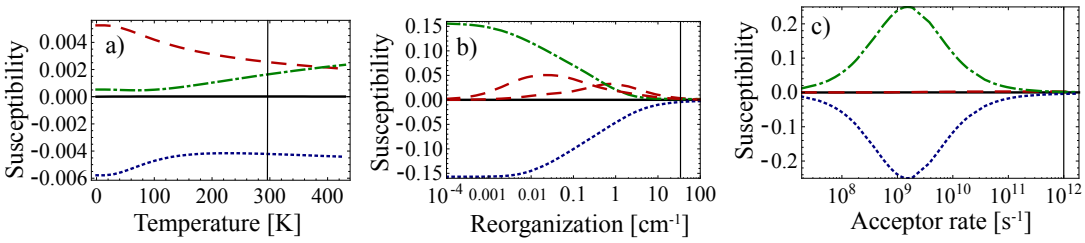

FIG. 3: Susceptibility versus a) temperature, b) reorganization energy (log-linear), and c) transfer rate to the acceptor. The processes considered are free Hamiltonian (black), the phonon bath coupling (red), transfer to the acceptor (green), and the loss of the excitation (blue). The initial state is a mixture of 1 and 6, except for the jump susceptibility in b) which is separated into 1 and 6 respectively. Standard parameters (shown as vertical lines) are $E_R = 35\text{cm}^{-1}$, $T = 295\text{K}$, $\kappa_3 = 1\text{ps}^{-1}$, and $\gamma^r = 1\text{ns}^{-1}$. For the standard parameters, the FMO complex shows relatively small susceptibilities, suggesting robustness with respect to external or evolutionary perturbations.

$\Gamma^p(n,m,m,n)(W^*_{m,n} \otimes W_{n,m})$, in the quantum walk master Eq. (10). We obtain a schematic picture of the most susceptible pathways in the FMO complex. The susceptibilities are correlated with the incoherent transport pathways. The susceptibilities are large when relaxation or absorption of energy due to the phonon bath is important for a particular transport pathway. This is the case e.g. when there is a relatively large off-resonance between different sites and thus coherent coupling does not lead to significant overlap between the sites, for example for sites 3/7. On the other hand, when coherent coupling is similar to the site-energy splitting, incoherent processes are less significant, leading to small susceptibilities such as for sites 1/2 and 5/6. A positive (negative) susceptibility of a process Λ_{nm} indicates an increasing (decreasing) ETE. For the FMO complex, jumps towards (away from) site 3 have positive (negative) susceptibility, a signature of the directionality in the irreversible dynamics. Thus, the quantum walk formalism together with a rather straightforward measure of the energy transfer susceptibility provides a valuable method to investigate spatial exciton transfer pathways in multichromophoric arrays.

VI. CONCLUSIONS AND FUTURE WORK

We have developed a general theoretical framework within the Lindblad formalism for studying the role of quantum effects in energy transfer dynamics of arbitrary chromophoric arrays interacting with a thermal bath from a microscopic Hamiltonian. We have shown that a quantum walk approach, which has been widely used in quantum information science, provides an appropriate mathematical framework for studying energy transfer. We have generalized the concept of continuous-time quantum walks to non-unitary and temperature-dependent dynamics in Liouville space. This approach can also be used to generally study decoherence effects in quantum walks in arbitrary geometries. The energy transfer efficiency was used as a universal measure to study the transfer properties of the environment-assisted quantum walk. We We have applied our method to explore the energy transfer efficiency and its susceptibilities for the Fenna-Matthews-Olson protein complex as a function of temperature, reorganization energy, trapping rates, and quantum jumps. In particular the energy transfer susceptibilities were studied with respect to the free Hamiltonian, the phonon bath, dephasing, trapping rate, and the exciton loss. This approach provides valuable insight into the dynamical role of various generators of the master equation and into spatial exciton transfer pathways in multichromophoric arrays. We have shown that the overall environment coupling strength leads to a substantial enhancement of the ETE of about 25% for the FMO complex. Thus, the overall energy transfer efficiency of 99% can be explained with the open nature of the multichromophoric dynamics involving an effective interplay between free Hamiltonian and fluctuations in the protein and solvent.

We applied the general formalism presented in this work to reveal the contributions of underlying physical mechanism to quantum transport [50]. We also quantified the phenomena of environment-assisted quantum transport due to an effective interplay of quantum dynamical coherence and a pure-dephasing noise model [51]. Using pure dephasing model, others observed similar effects [52, 53]. Motivated by recent observations of non-local effects in the structure and the dynamics of the purple bacteria reaction center [22] and the FMO protein [48], and also based on recent advances in the understanding and control of non-Markovian open quantum systems [54, 55], generalizations of our scheme to include environments with temporal and spatial correlations are currently underway. These results could lead to new ways for engineering optimal state transfer in quantum spin networks [56, 57] which interact with realistic environments. Since we employ the Lindblad equation, our quantum walk formalism can be implemented numerically using the Monte Carlo wavefunction (MCWF) approach. The MCWF method was originally developed for dissipative processes in quantum optics [58]. The main advantage of MCWF is the fact that one only needs to simulate the wave function rather than the density operator [59]. Our approach can potentially be used to enhance energy transfer efficiency via engineering quantum interference effects. For certain binary tree chromophoric arrays, e.g., dendrimers, quantum walks could lead to an exponential speed-up over classical walks of excitations [30]. In general, the combined biology and quantum information inspired approach of this study could provide new insight for engineering

artificial photosystems, such as quantum dots and dendrimers [60] to achieve optimal energy transport by exploiting their environmental effects.

We would like to acknowledge useful discussions with J. Biamonte, G.R. Fleming, I. Kassal, A. Najmaie, A.T. Rezakhani, and L. Vogt. We thank the Faculty of Arts and Sciences of Harvard University, the Army Research Office (project W911NF-07-1-0304) and Harvard's Initiative for Quantum Science and Engineering for funding.

[1] R.E. Blankenship, *Molecular Mechanism of Photosynthesis* (Blackwell Science, London, 2002).
[2] X. Hu, T. Ritz, A. Damjanović , and K. J. Schulten, Phys. Chem. B **101**, 3854 (1997).
[3] T. Ritz, S. Park, and K. Schulten, J. Phys. Chem. B **105,** 8259 (2001).
[4] V. I. Novoderezhkin, M. A. Palacios, H. van Amerongen, R. van Grondelle, J. Phys. Chem. B **108**, 10363 (2004).
[5] M. Cho, H.M. Vaswani, T. Brixner, J. Stenger, and G.R. Fleming, J. Phys. Chem. B **109,** 10542 (2005).
[6] T. Förster, in *Modern Quantum Chemistry, Istanbul Lectures*, edited by O. Sinanoglu (Academic, New York, 1965), Vol. 3, pp. 93–137.
[7] G. D. Scholes, Annu. Rev. Phys. Chem. 54 , 57-87 (2003).
[8] V. May and O. Kuhn, *Charge and Energy Transfer Dynamics in Molecular Systems* (Wiley-VCH, Weinheim, 2004).
[9] A.G. Redfield, Adv. Magn. Reson. **1**, 1 (1965).
[10] M. Grover and R. Silbey, J. Chem. Phys. **54**, 4843 (1971).
[11] S. Rackovsky, R. Silbey, Mol. Phys. **25** 61 (1973).
[12] H. Haken and G. Strobl, Z. Phys. **262**, 135 (1973).
[13] V.M. Kenkre, R.S. Knox, Phys. Rev. Lett. **33** 803 (1974).
[14] V. M. Kenkre and P. Reineker, *Exciton Dynamics in Molecular Crystals and Aggregates* (Springer, Berlin, 1982).
[15] W. M. Zhang, T. Meier, V. Chernyak, S. Mukamel, J. Chem. Phys. **108**, 7763 (1998).
[16] M. Yang and G. R. Fleming, Chem Phys **275**, 355 (2002).
[17] S. Jang, M.D. Newton, and R.J. Silbey, Phys. Rev. Lett. **92**, 218301 (2004).
[18] Y. C. Cheng and R. J. Silbey, Phys. Rev. Lett. **96**, 028103 (2006).
[19] S. Jang, M. D. Newton, and R. J. Silbey, J. Phys. Chem. B **111**, 6807 (2007).
[20] K M. Gaab and C. J. Bardeen, J. Chem. Phys. **121**, 7813 (2004).
[21] G.S. Engel, T.R. Calhoun, E.L. Read, T.-K. Ahn, T. Mancal, Y-C. Cheng, R.E. Blankenship, and G.R. Fleming, Nature **446**, 782 (2007).
[22] H. Lee, Y.-C. Cheng, and G.R. Fleming, Science **316**, 1462 (2007).
[23] R. P. Feynman, R. B. Leighton, M. Sands, *The Feynman Lectures on Physics* (Addison Wesley, Reading, MA, 1964).
[24] R. P. Feynman and A. R. Hibbs, *Quantum Mechanics and Path Integrals* (McGraw-Hill, New York, 1965).
[25] J. Klafter and R. Silbey, Physics Letters, **76A**, 143 (1980).
[26] Y. Aharonov, L. Davidovich, and N. Zagury, Phys. Rev. A **48**, 1687 (1993).
[27] J. Kempe, Contemp. Phys. **44**, 302 (2003).
[28] V. Kendon, Math. Struct. Comp. Sci. **17**, 1169 (2006).
[29] E. Farhi and S. Gutmann, Phys. Rev. A **58**, 915 (1998).
[30] A. Childs, E. Farhi, and S. Gutmann, Quan. Info. Proc. **1**, 35 (2002).
[31] D. Aharonov, A. Ambainis, J. Kempe, and U. Vazirani, in *Proc. 33th STOC* (ACM, New York, 2001) p. 50.
[32] D. A. Meyer, J. Stat. Phys. **85**, 551 (1996).
[33] B.C. Sanders, S.D. Bartlett, B. Tregenna, and P.L. Knight, Phys. Rev. A; W. Dür, R. Raussendorf, V.M. Kendon, and H.-J. Briegel, Phys. Rev. A **66,** 052319 (2002).
[34] O. Muelken, V. Bierbaum, and A. Blumen, J. Chem. Phys. **124**, 124905 (2006).
[35] O. Flomenbom, R. J. Silbey, arXiv:0706.2328 (2007).
[36] P.W. Anderson, Phys. Rev. **109**, 1492 (1958).
[37] L. K. Grover, Phys. Rev. Lett. **79**, 325 (1997).
[38] Y. Li, W. Zhou, R. E. Blankenship, and J. P. Allen, J. Mol. Biol. **271,** 456 (1997).
[39] S. Mukamel, *Principles of Nonlinear Optical Spectroscopy* (Oxford University Press, New York, 1995).
[40] H. -P. Breuer and F. Petruccione, *The Theory of Open Quantum Systems* (Oxford Univerity Press, New York, 2002).
[41] T.G. Owens, S.P. Webb, L. Mets, R.S. Alberte, and G.R. Fleming, Proc. Natl. Acad. Sci. USA **84**, 1532 (1987).
[42] J. Adolphs and T. Renger, Biophys. J. **91,** 2778 (2006).
[43] M.K. Sener, D. Lu, T. Ritz, S. Park, P. Fromme, and K. Schulten, J. Phys. Chem. B **106,** 7948 (2002).
[44] M.K. Sener, S. Park, D. Lu, A. Damjanović, T. Ritz, P. Fromme, and K. Schulten, J Chem. Phys. **120,** 11183 (2004).
[45] H. Carmichael, *An Open Systems Approach to Quantum Optics* (Springer-Verlag, Berlin, 1993).
[46] A. Olaya-Castro, C. Fan Lee, F. Fassioli Olsen, and N. F. Johnson, arXiv:0708.0436.
[47] A. Nazir, B.W. Lovett, S.D. Barrett, J.H. Reina, and G.A.D. Briggs, Phys. Rev. B **71**, 045334 (2005).
[48] F. Müh, M. El-Amine Madjet, J. Adolphs, A. Abdurahman, B. Rabenstein, H. Ishikita, E.-W. Knapp, and T. Renger, Proc. Natl. Acad. Sci. USA **104**, 16862 (2007).
[49] A.N. Melkozernov, J.M. Olson, Y. Li, J.P. Allen, and R.E. Blankenship, Photosynthesis Research **56**, 315 (1998).
[50] P. Rebentrost, M. Mohseni, and A. Aspuru-Guzik, arXiv:0806.4725 (2008).
[51] P. Rebentrost, M. Mohseni, S. Lloyd, I. Kassal, and A. Aspuru-Guzik, arxiv:08070929 (2008).
[52] M.B. Plenio and S.F. Huelga, arXiv:0807.4902 (2008).
[53] F. W. Strauch, arXiv:0808.3403 (2008).
[54] P. Rebentrost, I. Serban, T. Schulte-Herbrueggen, and F.K. Wilhelm, arXiv:quant-ph/0612165 (2006).
[55] M. Mohseni, and A. T. Rezakhani, arXiv:0805.3188 (2008).
[56] M. Christandl, N. Datta, A. Ekert and A. J. Landahl, Phys. Rev. Lett. **92**, 187902 (2004).
[57] D.I. Tsomokos, M.B. Plenio, I. de Vega, S.F. Huelga, arXiv:0808.2261v (2008).
[58] J. Dalibard, Yvan Castin, Klaus Molmer, Phys. Rev. Lett. **68**, 580 (1992).
[59] S. Ohta, M. Nakano, R. Kishi, H. Takahashi, S. Furukawa, Chem Phys Letters **419**, 70 (2006).
[60] Z. He, T. Ishizuka, and D. L. Jiangi, Polymer J. **39**, 889 (2007).